theory.[16] The reduction in interligand repulsion by removal of electron density on the oxygen atoms may then be sufficient to overcome the usual strong preference for octahedral geometry.

The MO calculation[16] suggested that the trigonal prism should have slightly higher stability than the octahedron for a d^{10} ion, though this was considered to be an artefact of the method of calculation. However, it would be expected that the tendency to octahedral geometry would increase where crystal field effects enhance its stability. It is not surprising, therefore, that K[M(acac)$_3$] (M = Co and Ni) apparently have geometries close to octahedral. It seems, however, that with the stronger polarizing power of sodium cations, there may be an appreciable trigonal twist of the octahedron, since the D values are again very high for six identical donor atoms.

It is clear that the EPR signal of manganese(II) ions doped into the lattice gives a very sensitive method of detecting such deviations from idealized geometry. However, far more investigations on compounds of known structure are required in order to provide a basis for their interpretation. From the present work it seems likely that the observed negative value of D corresponds to a trigonally elongated arrangement of donor atoms, and, particularly, to a low value of the twist angle ϕ.[9]

Acknowledgment. We thank the University of London for a Postgraduate Studentship (to R.B.B.) and Dr. J. F. Gibson for the use of computer programs.

Registry No. K[Cd(acac)$_3$], 68566-67-6; Na[Cd(acac)$_3$], 68566-68-7; Na[Co(acac)$_3$], 20106-06-3; Na[Zn(acac)$_3$], 14589-37-8; Na[Ni(acac)$_3$], 42230-53-5; Mn(II), 16397-91-4.

References and Notes

(1) R. D. Dowsing, J. F. Gibson, D. M. L. Goodgame, M. Goodgame, and P. J. Hayward, *Nature (London)*, **219**, 1037 (1968).
(2) C. J. O'Connor and R. L. Carlin, *Inorg. Chem.*, **14**, 291 (1975).
(3) M. Goodgame and P. J. Hayward, *J. Chem. Soc. A*, 3406 (1971).
(4) R. B. Birdy and M. Goodgame, *J. Chem. Soc., Dalton Trans.*, 461 (1977).
(5) T. M. Greaney, C. L. Raston, and A. H. White, *J. Chem. Soc., Dalton Trans.*, 876 (1975).
(6) F. P. Dwyer and A. M. Sargeson, *J. Proc. R. Soc. N.S.W.*, **40**, 29 (1956).
(7) D. Vivien and J. F. Gibson, *J. Chem. Soc., Faraday Trans. 2*, 1640 (1975).
(8) J. F. Gibson and G. M. Lack, to be submitted for publication.
(9) E. I. Stiefel and G. F. Brown, *Inorg. Chem.*, **11**, 434 (1972).
(10) G. M. Woltermann and J. R. Wasson, *J. Phys. Chem.*, **77**, 945 (1973).
(11) M. Vijayan and M. A. Viswamitra, *Acta Crystallogr., Sect. B*, **24**, 1067 (1968).
(12) R. R. Sharma, *Phys. Rev. B*, **3**, 76 (1971).
(13) R. Chatterjee, M. R. Smith, and H. A. Buckmaster, *Can. J. Phys.*, **54**, 1224 (1976).
(14) J. C. Hempel, *J. Chem. Phys.*, **64**, 4307 (1976).
(15) R. Hultgren, *Phys. Rev.*, **40**, 891 (1932).
(16) R. Hoffmann, J. M. Howell, and A. R. Rossi, *J. Am. Chem. Soc.*, **98**, 2484 (1976).

Contribution from the Chemistry Department and Energy and Mineral Resources Research Institute,
Iowa State University, Ames, Iowa 50011, and the Chemistry Department, Auburn University, Auburn, Alabama 36830

Polarized Electronic Absorption Spectra for Dirhodium(II) Tetraacetate Dihydrate

DON S. MARTIN, JR.,*[1a] THOMAS R. WEBB,[1b] GARY A. ROBBINS,[1a] and PHILLIP E. FANWICK[1a]

Received July 7, 1978

Single-crystal polarized absorption spectra are reported for the $\bar{1}01$ face of $Rh_2(O_2CCH_3)_4{\cdot}2H_2O$ in the region of 15 500–30 000 cm^{-1} and at temperatures of 300 and 15 K. An absorption band with a maximum at 17 300 cm^{-1} possesses vibrational structure in the $\perp b$ polarization. It corresponds to molecular x,y polarization and has been assigned as Rh–Rh $\pi^* \rightarrow$ Rh–Rh σ^*. Weaker absorptions with maxima at 23 300 cm^{-1} in $\perp b$ and 22 200 cm^{-1} in $\| b$ indicate the presence of more than one transition in this region. Possible assignments for these transitions are discussed.

Introduction

Polarized electronic absorption spectra have been reported in recent years for a number of dimeric complexes of molybdenum[2–5] and rhenium[6,7] which possess multiple metal–metal bonds. The present work provides polarized spectra recorded at temperatures of ca. 300 and 15 K for single crystals of $Rh_2(O_2CCH_3)_4{\cdot}2H_2O$. Norman and Kolari[8] have recently completed an Xα scattered-wave computation for ground-state orbital energies of anhydrous and hydrated dirhodium(II) tetraformate, and they have reviewed rather well conflicting claims in the literature concerning the existence of a single or multiple rhodium–rhodium bond in this molecule. The crystal structure for the $Rh_2(O_2CCH_3)_4{\cdot}2H_2O$ is available from the X-ray diffraction study of Cotton et al.[9] The visible absorption bands of $Rh_2(O_2CCH_3)_4$ in H_2O as well as in a series of basic solvents have been listed by Johnson, Hunt, and Neuman.[10] In addition, Dubicki and Martin[11] have characterized the diffuse-reflectance spectrum for dirhodium(II) tetraacetate dihydrate, and a plot for the rhodium(II) isobutyrate was presented in this reference. An aqueous solution spectrum in the UV region down to 200 nm was also presented.

Experimental Section

Rhodium(II) acetate was prepared from rhodium(III) chloride by the method of Rempel et al.[12] and converted to the hydrate by recrystallizing from water.[9]

The procedure for recording crystal spectra has been described previously.[13]

Bulk samples of $Rh_2(O_2CCH_3)_4{\cdot}2H_2O$ were very dark green, nearly black. A number of crystals had the form of thin platelets with well-defined faces. The extinctions for these faces were observed between crossed polarizers of a polarizing microscope. It was noted that the crystals were distinctly dichroic. For one extinction the color was a blue-green (bg), whereas for the other extinction the color was a yellow-green (yg). A crystal plate was found which would stand on edge so its thickness could be measured by a calibrated scale in the microscope eyepiece. Its thickness was 32 ± 3 μm. This crystal was mounted over a pinhole, and the polarized spectra shown in Figure 1 were recorded from ca. 580 to 325 nm for room temperature and with liquid helium in the cryostat. Since the cooling was by conduction, and the temperature of the sample could not be measured, the temperature has been assigned, conservatively it is believed, as 15 K.

After the spectra were recorded, this crystal was cemented to a glass fiber which was mounted on the goniometer head of a four-circle diffractometer. Ten reflections were obtained from oscillation photographs and refined. From these reflections the cell parameters were calculated by standard programs to be $a{:}b{:}c$ = 13.25:8.59:13.97 and $\alpha{:}\beta{:}\gamma$ = 90.06:117.19:89.96. These were in excellent agreement with the reported parameters for a monoclinic cell[9] $a{:}b{:}c$ = 13.287:8.608:14.042 and β = 117.23°. Various planes of the crystal were called into the diffracting position, and it was observed that the large faces of this crystal were $\bar{1}01$ planes. It was also noted that the unique monoclinic axis, b, lay in the direction of the yellow-green extinction. Accordingly, the yg extinction has been designated as $\| b$ and the bg extinction has been labeled as $\perp b$ for this $\bar{1}01$ face.

A second crystal was found which was much thinner than the first. Its thickness was estimated to be 5.2 μm by comparison of its peak height at ca. 23 000 cm^{-1} in the $\| b$ polarization with the peak of the

0020-1669/79/1318-0475$01.00/0

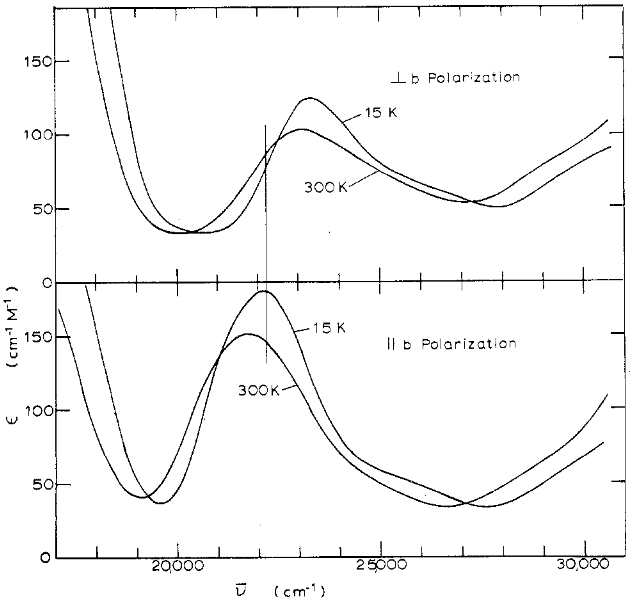

Figure 1. Polarized crystal spectra for the 22 000–23 000-cm^{-1} bands of $Rh_2(O_2CCH_3)_4 \cdot 2H_2O$. Crystal thickness was 32 μm.

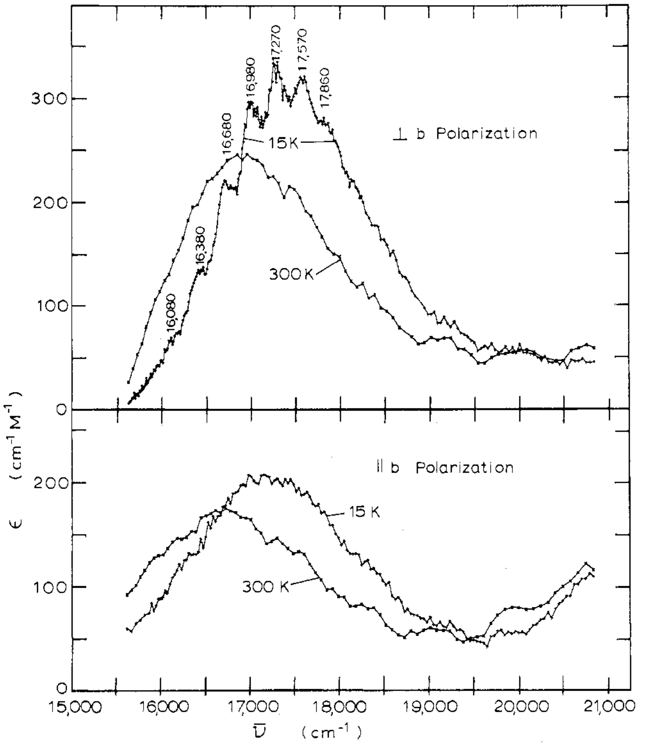

Figure 2. Polarized crystal spectra for the 17 000-cm^{-1} band of $Rh_2(O_2CCH_3)_4 \cdot 2H_2O$. Crystal thickness was 5.2 μm.

first crystal. Polarized spectra for this second crystal could be extended to 640 nm, and its spectra in the region of 15 500–21 000 cm^{-1} are presented in Figure 2.

Results and Discussion

The ground-state orbital energies in the spectroscopically accessible region, calculated with the Xα scattered-wave technique of Norman and Kolari,[8] are shown to scale in Figure 3 for the dimolybdenum(II) tetraformate dihydrate molecule. For these calculations they assumed that the planes defined by the terminal water molecules bisected the two planes defined by the metal–metal bond and the CCO_2 framework of the acetate molecules. With this configuration the point group symmetry would be D_{2h}, and the irreducible representations for the orbitals are shown in Figure 3 for D_{2h} as well as under the D_{4h} point group which would apply to a nonhydrated molecule. The computations predicted splitting of the degenerate orbitals of D_{4h} by 0.15–0.20 eV under the D_{2h} structure.

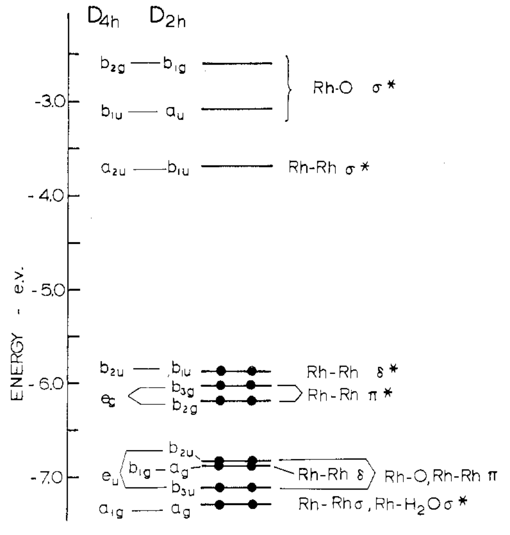

Figure 3. Orbital energies for $Rh_2(O_2CH)_4 \cdot 2H_2O$ from Xα scattered-wave calculations of Norman and Kolari.[8] Note the *x* and *y* axes lie in the planes which bisect the angles between the acetate ligand planes.

The highest occupied orbital was the Rh–Rh δ* ($b_{2u}(D_{4h})$), and the Rh–Rh π* ($e_g(D_{4h})$) was only slightly lower and split into b_{2g}, b_{3g} under D_{2h}. The lowest unoccupied orbital was the Rh–Rh σ* ($a_{2u}(D_{4h})$), and the next higher orbital was a Rh–O σ* ($b_{1u}(D_{4h})$). Thus, the calculation indicates filled metal–metal π* and δ* orbitals and therefore effectively a single metal–metal bond. It is noteworthy that the δ* orbital lies above the π* orbitals.

Norman and Kolari assigned the solution bands at 17 100 and 22 700 cm^{-1} to the *x,y* dipole-allowed transitions Rh–Rh π* ($e_g(D_{4h})$) → Rh–Rh σ* ($a_{2u}(D_{4h})$) and Rh–Rh π* ($e_g(D_{4h})$) → Rh–O σ* ($b_{1u}(D_{4h})$) on the basis of their energy computations and the observation that the 17 100-cm^{-1} band is more blue-shifted by stronger axial donors than the 22 700-cm^{-1} band.

Considerations of the Crystal Structure. The crystals of $Rh_2(O_2CCH_3)_4 \cdot 2H_2O$ conform to the space group *C*2/*c* with four molecules per unit cell. However, since this structure has a *C*-face-centered structure, there are only two molecules per primitive cell, and there will be only two Davydov states for each molecular transition. For the $\bar{1}01$ face, transitions to one of the Davydov states for a molecular transition will be forbidden in ‖*b* polarization, and the other will be forbidden in ⊥*b* polarization. The site symmetry is only $\bar{1}$.

Polarization ratios for the $Rh_2(O_2CCH_3)_4 \cdot 2H_2O$ transitions have been calculated on the basis of oriented noninteracting gas molecules. If the electronic transitions were restricted to the region where a local D_{4h} symmetry was maintained, dipole-allowed transitions would occur either with *z* polarization or as degenerate pairs with *x,y* polarization. The *z* or fourfold symmetry axis lies along the metal–metal bond. This bond lies at an angle, θ_1, of 57.46° with the *b* axis and at an angle, θ_2, of 91.95° with the ⊥*b* extinction direction. If molar absorptivities of ϵ_π and ϵ_σ apply to the molecular *z* and *x,y* polarizations, respectively, $\epsilon_{\parallel b}$ and $\epsilon_{\perp b}$ for the crystal orientations of the molecules are given in matrix form by[14]

$$\begin{bmatrix} \epsilon_{\parallel b} \\ \epsilon_{\perp b} \end{bmatrix} = \begin{bmatrix} \cos^2\theta_1 & \sin^2\theta_1 \\ \cos^2\theta_2 & \sin^2\theta_2 \end{bmatrix} \begin{bmatrix} \epsilon_\pi \\ \epsilon_\sigma \end{bmatrix}$$

It was calculated from the expression that the polarization ratio

($\epsilon_{\|b}/\epsilon_{\perp b}$) would be 249 for a z-polarized molecular transition and 0.7115 or 1/1.465 for an x,y-polarized transition.

In case the symmetry of the molecule has been effectively reduced to the D_{2h} utilized by Norman and Kolari,[8] the degenerate x,y-polarized transitions could be split in energy, and the two molecular transitions would be separately polarized along x and y axes. Molecular orthogonal x and y axes were therefore defined by vectors orthogonal to the metal–metal bond and each lying in the plane containing the metal–metal bond and bisecting the angle formed by vectors from the origin and the carboxyl carbon atoms. The x axis formed an angle of 67.03° with b and an angle of 26.39° with the $\perp b$ extinction direction while the y axis formed an angle of 41.65° with b and 63.69° with the $\perp b$ extinction. Thus, the x-polarized transition would give 15.2% of its intensity $\|b$ and 80.2% $\perp b$ for a polarization ratio of 0.189. The y-polarized transition would yield 55.8% of its intensity $\|b$ and 19.6% $\perp b$ for a polarization ratio of 2.84.

Crystal Spectra. The low-energy band, Figure 2, has a maximum at 16 800 cm^{-1} at room temperature. The absolute intensities were not determined accurately since it was not possible to scan into a wavelength region of negligible absorption, and the zero absorption must be set arbitrarily. However, it is clear that the integrated absorption does not fall off appreciably as would be expected for a dipole-forbidden transition which gains its intensity from a vibronic perturbation. The fact that the $\perp b$ intensity is somewhat greater than $\|b$ would be consistent with x,y rather than z polarization. Vibrational structure is clearly evident in the $\perp b$ polarization, but no structure is discernible above the noise for $\|b$ polarization. The maximum in the $\|b$ polarization at helium temperature is 17 300 cm^{-1} and coincides with the highest vibrational line in $\perp b$ polarization so there would be no energy splitting of the x and y polarizations indicated by these maxima. It is possible that the splitting of x- and y-polarized transitions is of the order of half the vibrational splitting of the transition. Since the $\|b$ polarization is composed of somewhat more nearly equal fractions of the two transitions, the height of the vibrational peaks would be reduced although the lower intensity would be a factor as well. Seven vibrational components were distinguishable in the helium $\perp b$ spectrum. The average of the six spacings was 297 ± 5 cm^{-1}.

All of the above features appear to be consistent with Norman and Kolari's assignment of this band as Rh–Rh π^* ($e_g(D_{4h})$) → Rh–Rh σ^* ($a_{2u}(D_{4h})$). The intensity is low for a dipole-allowed transition and especially in comparison with the $\delta^* \leftarrow \delta$ of dimeric Mo^{II} complexes. However, the transition requires a rhodium–rhodium electron transfer, and a low intensity should result from the relatively long metal–metal bond distance of 2.38 Å. The separation of the terms in Franck–Condon progression of 297 cm^{-1} is expected to describe the metal–metal stretching vibration in the excited electronic state. This value can be compared to 320 cm^{-1} for the ground state available from the Raman spectrum[15] of $Rh_2(O_2CCH_3)_4 \cdot 2H_2O$. The reduction in frequency for the excited state would result from relaxation of the bond as an electron is transferred from π^* to the more effective antibonding σ^* orbitals.

The absorption in the vicinity of 21 000–25 000 cm^{-1}, Figure 1, is much less intense than that for the lower energy band. Furthermore, the maximum of the peak (22 000 cm^{-1}) in $\|b$ is some 1100 cm^{-1} lower than the peak in $\perp b$ polarization. The $\|b$-polarized peak is more intense than that for $\perp b$ polarization. Norman and Kolari assigned the absorption in this region to the transitions Rh–Rh π^* ($e_g(D_{4h})$) → Rh–O σ^* (b_{1u}). Somewhat lower intensity for this transition should occur because the electron transfer is from one rhodium atom into the antibonding Rh–O orbital on the other rhodium. Since the D_{2h} splitting of the degenerate π^* ($e_g(D_{4h})$) orbitals could not be seen in the 17 300 cm^{-1} band, it does not appear that it can account for separation in the maxima in this region. Therefore it is concluded there must be an additional transition contributing to the intensity in this region.

According to Figure 3 the $b_{2u}(D_{4h})$ orbital lies just above the Rh–Rh π^* orbitals. Thus the dipole-forbidden transition Rh–Rh δ^* ($b_{2u}(D_{4h})$) → Rh–O σ^* ($b_{1u}(D_{4h})$) might lie in just this region. This dipole-forbidden transition could receive intensity from vibronic perturbations. Since this transition is $^1A_{1g} \rightarrow {}^1A_{2g}$, A_{1u} and E_u vibrations would provide intensity for z and x,y polarization, respectively. An Rh_2O_8 framework under D_{4h} symmetry has three A_{1u} and three E_u pairs of vibrations. However, the temperature dependence of this peak does not have the form of a vibronically excited band. Clearly, the intensity of the $\|b$-polarized component at 22 200 cm^{-1} has not fallen off upon cooling the crystal from 300 to 15 K as would be expected for a vibronically excited band. Professor Joe G. Norman has suggested that this transition might possibly be Rh–Rh δ ($b_{1g}(D_{4h})$) → Rh–Rh σ^* ($a_{2u}(D_{4h})$) transition. This transition would be dipole forbidden under D_{4h}. However, under D_{2h} it is $a_g \rightarrow b_{1u}$, and it is dipole allowed with z polarization. This would account for its much higher intensity in the $\|b$ polarization over that in $\perp b$.

The location of the Rh–Rh δ^* ($b_{2u}(D_{4h})$) orbital suggests that there should also be a dipole-forbidden vibronically allowed transition just below the Rh–Rh π^* → Rh–Rh σ^* transition at 17 300 cm^{-1}. We were not able to extend our measurements below 15 500 cm^{-1} because of the decrease in sensitivity of the detector in the spectrophotometer. However, evidence for such a weak transition[11] can be seen in the diffuse-reflectance spectrum of rhodium(II) isobutyrate where there is a weak shoulder at 14 300 cm^{-1} on a peak at 16 500 cm^{-1}.

With the presence of two transitions of comparable energy in the region of 22 000–23 500 cm^{-1} it is not possible to specify the energy of either accurately. It does appear that they must be separated by 1500–2000 cm^{-1}. A weak shoulder occurs at about 26 000 cm^{-1} in each polarization. This might possibly be a forbidden transition from one of the lower set of Rh–Rh δ, or Rh–Rh π, and Rh–O $\pi \rightarrow \sigma^*$. Any one of these transitions would be dipole forbidden even under D_{2h}.

The polarized crystal spectra appear, therefore, to be in general agreement with the computations and assignments, although perhaps the splitting of the degeneracies under D_{4h} upon reduction in symmetry by the terminal waters is not as great as computed.

Acknowledgment. We wish to thank Professor J. G. Norman for providing us with his paper prior to publication and for his helpful suggestions. This work was supported in part by the Energy and Mineral Resources Research Institute of Iowa State, in part by National Science Foundation Grant CHE-76-83655, and in part by the Auburn University Grant-in-Aid Program.

Registry No. $Rh_2(O_2CCH_3)_4 \cdot 2H_2O$, 29998-99-0.

References and Notes

(1) (a) Iowa State University. (b) Auburn University.
(2) F. A. Cotton, D. S. Martin, T. R. Webb, and T. J. Peters, *Inorg. Chem.*, **15**, 1199 (1976).
(3) F. A. Cotton, D. S. Martin, P. E. Fanwick, Timothy J. Peters, Thomas R. Webb, *J. Am. Chem. Soc.*, **98**, 4681 (1976).
(4) W. C. Trogler, E. I. Solomon, I. Trajberg, C. J. Ballhausen, and H. B. Gray, *Inorg. Chem.*, **16**, 828 (1977).
(5) P. E. Fanwick, D. S. Martin, F. A. Cotton, and T. R. Webb, *Inorg. Chem.*, **16**, 2103 (1977).
(6) C. D. Cowman and H. B. Gray, *J. Am. Chem. Soc.*, **95**, 8177 (1973).
(7) W. C. Trogler, C. D. Cowman, H. B. Gray, and F. A. Cotton, *J. Am. Chem. Soc.*, **99**, 2993 (1977).
(8) J. G. Norman and H. J. Kolari, *J. Am. Chem. Soc.*, **100**, 791 (1978).
(9) F. A. Cotton, B. G. DeBoer, M. D. LaPrade, J. R. Pipal, and D. A. Ucko, *Acta Crystallogr., Sect. B*, **27**, 1664 (1971).

(10) S. A. Johnson, H. R. Hunt, and H. M. Neuman, *Inorg. Chem.*, **2**, 960 (1963).
(11) L. Dubicki and R. L. Martin, *Inorg. Chem.*, **9**, 673 (1970).
(12) G. A. Rempel, P. Legzdins, H. Smith, and G. Wilkinson, *Inorg. Synth.*, **13**, 90 (1972).
(13) D. S. Martin, Jr., *Inorg. Chim. Acta, Rev.*, **5**, 107 (1971).
(14) This matrix, although in somewhat different form, is equivalent to the one presented by T. S. Piper, *J. Chem. Phys.*, **35**, 1240 (1961).
(15) A. P. Ketteringham and C. Oldham, *J. Chem. Soc., Dalton Trans.*, 1067 (1973).

Contribution from the Departments of Chemistry, The Pennsylvania State University, University Park, Pennsylvania 16802, and Northern Illinois University, DeKalb, Illinois 60115

Metal-to-Ligand Charge-Transfer Spectra of Some Chloro-Bridged Complexes of Rhodium(I) and Iridium(I)

RONALD A. EPSTEIN,[1a] GREGORY L. GEOFFROY,*[1a] MARK E. KEENEY,[1a] and W. ROY MASON*[1b]

Received July 7, 1978

Electronic absorption and magnetic circular dichroism (MCD) spectra are reported for the chloro-bridged dimers $[RhCl(CO)_2]_2$, $[RhCl(COD)]_2$, $[RhCl(NBD)]_2$, and $[IrCl(COD)]_2$ (COD = 1,5-cyclooctadiene; NBD = norbornadiene) in dichloromethane solution. Absorption spectra are also reported for the less stable $[RhCl(C_2H_4)_2]_2$, $[RhCl(COT)_2]_2$, and $[IrCl(COT)_2]_2$ (COT = cyclooctene) complexes. Spectra at 77 K were also obtained for $[RhCl(CO)_2]_2$ and several of the olefin complexes in glassy EPA or methylcyclohexane/pentane solution. Dissolution of $[RhCl(CO)_2]_2$, $[RhCl(COD)]_2$, $[RhCl(NBD)]_2$, and $[IrCl(COD)]_2$ in acetonitrile gives a bridge-cleavage reaction, and spectral data are reported for the monomeric products $[RhCl(CO)_2(CH_3CN)]$, $[RhCl(COD)(CH_3CN)]$, $[RhCl(NBD)(CH_3CN)]$, and $[IrCl(COD)(CH_3CN)]$. The intense bands observed in the visible and near-ultraviolet regions of the spectra of all these complexes are assigned as metal-to-ligand charge-transfer (MLCT) transitions from occupied metal d orbitals to low-energy ligand π^* orbitals. Detailed spectral assignments are presented, and comparisons are made between the chloro-bridged complexes and related monomeric complexes.

Introduction

We have recently examined the electronic absorption and magnetic circular dichroism (MCD) spectra of a series of planar d^8 complexes possessing π-acceptor ligands.[2-6] These studies have included complexes of Rh(I), Ir(I), Pd(II), and Pt(II) with ligands such as CN^-, CNR, CO, PR_3, AsR_3, and bidentate diphosphines. The low-lying bands of these complexes in the visible–near-UV spectral region have been attributed to metal-to-ligand charge-transfer (MLCT) transitions.[2-6] To further our understanding of MLCT transitions in low-valent organometallic complexes we have turned our attention to a series of chloro-bridged dimeric complexes of Rh(I) and Ir(I), many of which possess olefinic ligands. These complexes afford us the opportunity to probe the effect of the dimerization on the MLCT transitions and, further, to examine the nature of metal-to-olefin charge transfer.

The complex which we have focused most of our attention on and discuss in detail herein is $[RhCl(CO)_2]_2$. X-ray structural analysis[7] of this complex has shown it to have the bent structure shown in **1** with the two $RhCl_2(CO)_2$ planes intersecting at an angle of 124°. The *intra*molecular Rh–Rh distance is 3.12 Å, and an *inter*molecular Rh–Rh contact distance of 3.31 Å was evident between dimeric units. Infrared spectral studies[8] and dipole moment measurements[9] showed that the complex maintains its bent geometry in solution, and hence the bending must not be due to crystal packing forces but must have an electronic origin. The nature of these effects was explored in a recent SCF–Xα–SW analysis by Norman and Gmur,[10] who concluded that there is no Rh–Rh interaction through the highest occupied set of mainly 4d orbitals and that the nonlinear geometry is due to interaction of orbitals that are mainly chlorine 3p in character.

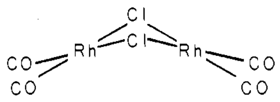

1

Of the several chloro-bridged olefin complexes which have been characterized, only two have had their structures determined by X-ray diffraction. The ethylene complex $[RhCl(C_2H_4)_2]_2$ has the bent geometry shown in **2**,[11] whereas $[RhCl(COD)]_2$ (COD = 1,5 cyclooctadiene) is planar with the olefinic bonds perpendicular to the Rh_2Cl_2 plane, **3**.[12]

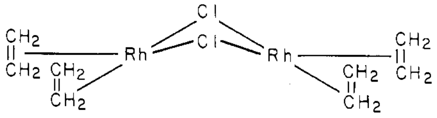

2

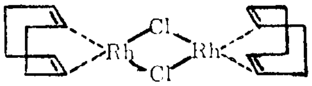

3

Definitive structural data for $[RhCl(NBD)]_2$ (NBD = norbornadiene), $[RhCl(COT)_2]_2$ (COT = cyclooctene), $[IrCl(COD)]_2$, and $[IrCl(COT)_2]_2$ are lacking. To our knowledge no information concerning solution geometries of any of these olefin complexes has been reported.

Experimental Section

The complexes $[RhCl(COD)]_2$,[13] $[RhCl(NBD)]_2$,[14] $[RhCl(COT)_2]_2$,[15] $[RhCl(C_2H_4)_2]_2$,[16] $[RhCl(CO)_2]_2$,[16] $[(n\text{-}C_4H_9)_4N][RhCl_2(CO)_2]$,[17] $[IrCl(COD)]_2$,[18] and $[IrCl(COT)_2]_2$[18] were prepared by published procedures. Electronic absorption spectra were recorded on a Cary Model 17 or a Cary Model 1501 spectrophotometer using 1.0-cm path length quartz cells. The MCD spectra were recorded on a Jasco ORD/uv-5 (equipped with CD attachment) using a permanent magnet (field 10^4 G). Spectra at 77 K were measured in frozen 5:5:2 diethyl ether/isopentane/ethanol (EPA) or 7:4 methylcyclohexane/pentane solutions using a quartz Dewar. The 77 K spectra were corrected for 26 and 20% solvent contraction, respectively.

Solutions of $[RhCl(C_2H_4)_2]_2$, $[RhCl(COT)_2]_2$, $[IrCl(COD)]_2$, and $[IrCl(COT)_2]_2$ were found to be quite air sensitive and were therefore prepared on a vacuum line or in an inert-atmosphere drybox using specially constructed degassable quartz UV cells or quartz tubes. Solvents for these solutions were dried using standard methods and degassed before use.

$[RhCl(COT)_2]_2$ rapidly decomposes even in degassed CH_2Cl_2 solution. We found that the decomposition could be slowed long enough to allow spectral measurements by adding excess COT to the solutions. However, reliable extinction coefficients and the low-temperature spectrum could not be obtained.[19] $[IrCl(COT)_2]_2$ proved to be more stable than $[RhCl(COT)_2]_2$, and degassed CH_2Cl_2 solutions

0020-1669/79/1318-0478$01.00/0